

MuxViz: a tool for multilayer analysis and visualization of networks

MANLIO DE DOMENICO*

*Departament d'Enginyeria Informática i Matemàtiques, Universitat Rovira I Virgili,
43007 Tarragona, Spain*

*Corresponding author. Email: manlio.dedomenico@urv.cat

MASON A. PORTER

*Oxford Centre for Industrial and Applied Mathematics, Mathematical Institute, University of Oxford,
Oxford OX2 6GG, UK and CABDyN Complexity Centre, University of Oxford, Oxford OX1 1HP, UK*

AND

ALEX ARENAS

*Departament d'Enginyeria Informática i Matemàtiques, Universitat Rovira I Virgili,
43007 Tarragona, Spain*

Edited by: Vito Latora

[Received on 26 May 2014; accepted on 23 July 2014]

Multilayer relationships among entities and information about entities must be accompanied by the means to analyse, visualize and obtain insights from such data. We present open-source software (`muxViz`) that contains a collection of algorithms for the analysis of multilayer networks, which are an important way to represent a large variety of complex systems throughout science and engineering. We demonstrate the ability of `muxViz` to analyse and interactively visualize multilayer data using empirical genetic, neuronal and transportation networks. Our software is available at <https://github.com/manlius/muxViz>.

Keywords: multilayer networks; software; visualization; multiplex networks; interconnected networks.

1. Introduction

Although the study of networks is old, the analysis of complex systems has benefited particularly during the last two decades from the use of networks to model large systems of interacting agents [1]. Such efforts have yielded numerous insights in many areas of science and technology [2–16].

In the case of biological networks, connections among genes, proteins, neurons and other biological entities can indicate that they are part of the same biological pathway or exhibit similar biological functions. Network representations focus on connectivity, and they have now become a paradigmatic way to investigate the organization and functionality of cells [17–26], synaptic connectivity [27–36] and more. There are also myriad applications to other types of systems (e.g. in sociology, transportation, physics and more) [1,37–41].

In parallel, a large variety of computational techniques have been developed to analyse (and visualize) networks and the information that they encode. In biology, for example, such methods have become important tools for attempting to understand and represent cell functionality. However, although the standard network paradigm has been very successful, it has a fundamental flaw: it forces the aggregation

of multilayer information to construct network representations that include only a single type of connection between pairs of entities. This can lead to misleading results, and it is becoming increasingly apparent that a more complicated representation is necessary [41].

Recently, a novel mathematical framework to model and analyse multilayer relationships and their dynamics was developed [42,43]. In this framework, one represents the underlying network topology and interaction weights as a *multilayer network*, in which entities can exhibit different relationships simultaneously and can exist on different ‘layers’. Multilayer networks can encode much richer information than what is possible using the individual layers separately (which is what is usually done). This, in turn, provides a suitable framework for versatile and sophisticated analyses that have already been used successfully to reveal multilayer community structure [42] and to measure important nodes and the correlations between them [43–46]. However, to meet the requirements of an operational toolbox to be applied to the analysis of complex systems, it is of paramount importance to also develop open-source software to visualize multilayer networks and to represent the results of analysing such networks in a meaningful way.

Multilayer networks have already yielded fascinating insights and are experiencing burgeoning popularity. For example, there have been numerous studies to attempt to understand how interdependencies [47,48], other multilayer structures [44–46,49–53], dynamics [54–58] and control [59] can improve understanding of complex interacting systems. See the recent review article [41] for extensive discussions and a thorough review of results.

The use of increasingly complicated network representations has yielded a new set of challenges: how should one visualize, analyse and interpret multilayer data. Although there has been progress in numerous applications, many of the key results have concentrated on data from examples like social and transportation networks [41]. Multilayer analysis has rarely been exploited in the investigation of biological networks—even though such a perspective is clearly relevant—and we believe that the lack of appropriate software has contributed to this situation. For example, in a recent study, the genetic and protein–protein interaction networks of *Saccharomyces cerevisiae* were investigated simultaneously [26] to uncover connection patterns. Costanzo *et al.* [26] also reported that genetic interactions have an overlap of 10–20% with protein–protein interaction pairs, which is significantly higher than the 3% overlap that they expected based on a random null model. This suggests that many positive and negative interactions occur between—rather than within—complexes and pathways [26] and thereby gives an important example of how exploiting multilayer information might improve understanding of biological structure and functionality.

The aforementioned overlap is an indication of correlation between a pair of networks, and the analysis of multilayer data would benefit greatly from techniques and diagnostics that are able to exploit multiplexity (i.e. multiple different ways to interact) in available information.

2. Methods

The primary contributions of the present work are to address the computational challenge of analysis and visualization of multilayer information by providing a practical methodology, and accompanying software that we call *muxViz*, for the analysis and the visualization of multilayer networks. In the appendix, we give technical details about the *muxViz* software.

2.1 Visualization

In multilayer networks, nodes can exist in several layers simultaneously, and entities that exist in multiple layers (such nodes have ‘replicas’ on other layers) are connected to each other via interlayer edges.

One can visualize a multilayer network in *muxViz* either using explicit layers or as an edge-coloured multigraph [41], in which edges are ‘coloured’ according to the different types of relationships that they represent. See Fig. 1 for examples of genetic and neuronal multilayer networks.

The *muxViz* software focuses predominantly on ‘multiplex networks’, which refer to networks with multiple relational types and which are arguably the most important (and prevalent) type of multilayer network. A large variety of systems in the biological, social, information, physical and engineering sciences can be described as multiplex networks. In *muxViz*, we consider two different types of interlayer connectivity: *ordinal* and *categorical*. In ordinal multilayer networks, interlayer edges exist only between layers that are adjacent to each other with respect to some criterion (e.g. temporal ordering). In contrast, categorical multilayer networks include interlayer edges between replica nodes from every pair of layers. For the sake of simplicity, we illustrate *muxViz* using interlayer edges of weight 1 in the present paper. In general, how to choose such weights is an open research question. See the discussions in Refs. [41,60].

For instance, let us examine the genetic-interaction and profile-correlation networks of a cell as different layers of a multilayer network. Such networks were aggregated into a single network in Ref. [26].

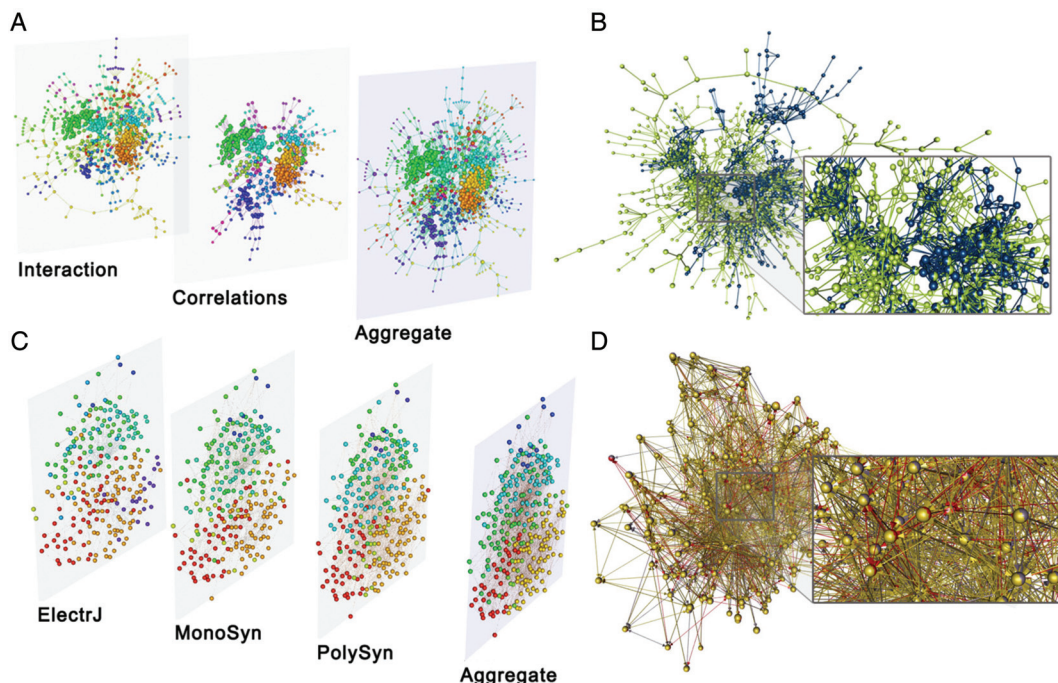


FIG. 1. Multilayer representations of genetic and neuronal networks. (A) Multilayer representation, in which the layers correspond to an interaction network of genes in *S. cerevisiae* (which was obtained via a synthetic genetic-array methodology) and a correlation-based network in which genes with similar interaction profiles are connected to each other. [The data come from Ref. [26].] In the third layer, we show an aggregated network. In this visualization, the colour of the nodes is their module assignment from multilayer community detection (see the text for further details). (B) Representation of the same network as an edge-coloured multigraph. (C) Multilayer and (D) edge-coloured-multigraph representations of the *C. elegans* connectome, where layers correspond to different synaptic junctions: electric ('ElectrJ'), chemical monadic ('MonoSyn') and polyadic ('PolySyn'). [The data come from Ref. [24].] In (B) and (D), we colour the nodes according to the layer to which they belong. If a node is part of multiple layers simultaneously, then we use an equal distribution of the corresponding colours for the node.

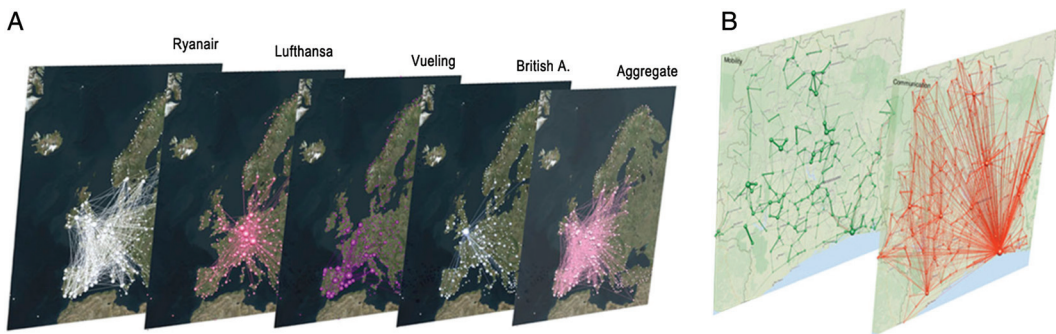


FIG. 2. Multilayer networks embedded in geographical regions. (A) Network of European airports, where each layer represents a different airline [51]. (B) Network of mobility and communication in the Ivory Coast, where nodes are geographical districts [63]. We used *muxViz* to visualize these data sets.

In Fig. 1(A), we show multilayer visualizations that we created using *muxViz*. Other representations are also possible [41]. For example, when representing these data as an edge-coloured multigraph, we ‘colour’ edges according to the type of relationship that they represent (see Fig. 1(B)). In Fig. 1(C and D), we show two visualizations for the connectome of *Caenorhabditis elegans*. In this example, each layer corresponds to a different type of synaptic connection [24].

In panels (A) and (C) of Fig. 1, we use a layout in which the positions of the nodes are the same in each layer. We determine the positions of nodes by combining two of the standard force-directed algorithms available in *muxViz* and applying them to an aggregated network that we obtained by summing the corresponding entries of the adjacency matrices of the individual layers. Specifically, we first apply the Fruchterman–Reingold algorithm [61] to the aggregated network and then use the output of this algorithm as a seed layout for the Kamada–Kawai algorithm [62] to achieve a better spatial separation of nodes in the final layout. The *muxViz* software also allows other layout choices. For example, the layout of each layer can be independent, or one can determine node locations using any individual layer or an aggregation over any subset of layers.

One can also use *muxViz* for a large variety of other analyses and visualizations. For example, as we illustrate in Fig. 2, *muxViz* can account for spatial information by creating visualizations of multilayer networks that are embedded in geographical regions. Moreover, *muxViz* allows one to produce animated visualizations of dynamical processes on top of multiplex networks. For instance, it is possible to visualize the movement of one or more random walkers in a network, the spreading of contagions or memes in a multiplex social network, traffic (and possible congestion) in a multiplex transportation or communication network, and more. With an appropriate input, it is possible to render animated visualizations of time-varying multiplex networks, in which nodes and/or edges can appear or disappear over time. (See the *muxViz* website for detailed instructions.)

2.2 Compression of layers and reducibility dendrograms

An important open question is the determination of how much information is necessary to accurately represent the structure of multilayer systems and whether it is possible to aggregate some layers without loss of information. It was shown recently that it is possible to compress the number of layers in multilayer networks in a way that minimizes information loss by using an information-theoretic approach [64]. The methodology of [64], which we implemented in *muxViz*, amounts to a tradeoff

(which is ‘optimal’ in some sense) between accuracy and complexity. Alternatively, users of *muxViz* can implement alternative methods based on different notions of ‘minimal information loss’.

The compression procedure from [64] proceeds as follows. For each pair of layers in the original multilayer network, *muxViz* calculates the quantum Jensen–Shannon (JS) divergence [65]. This estimates the similarity between two networks based on their Von Neumann entropy [66]. By definition, the quantum Jensen–Shannon divergence is symmetric and its square root, which is usually called the Jensen–Shannon distance, satisfies the properties of a metric [67]. One can use the JS distance to quantify the distance in terms of information gain (or loss) between the normalized Laplacian matrices that are associated to two distinct networks [64].

One uses the distances between every pair of layers as the components of a matrix, and one can then perform hierarchical clustering [68] using any desired method to produce a dendrogram that indicates the relatedness of the information in the different layers. In *muxViz*, we have included several methods for hierarchical clustering (e.g. Ward, McQuitty, single, complete, average, median and centroid linkage clusterings). We show an example of such a ‘reducibility dendrogram’ in panel (D) of Figs. 3, 5, 7 and 9. A reducibility dendrogram results from a step-by-step merging of a set of layers in a multilayer network, and we calculate a quality function based on the relative Von Neumann entropy to estimate information gain (or loss) at each step [64]. To obtain a reduced version of the original multilayer network, we stop the merging procedure at the level of the hierarchy that maximizes the relative entropy.

2.3 Annular visualization of multilayer information

It is a challenging problem to represent, visualize and analyse the wealth of information encoded in the multilayer structure of networks in a compact way. Preserving more information by using multilayer networks rather than ordinary networks complicates the visualization and analysis even further. However, this complication is necessary, because otherwise one might end up with misleading or even incorrect results [41]. We developed the *muxViz* software to help address these challenges. To summarize all of the information obtained from multilayer-network calculations in a compact way, *muxViz* includes an annular visualization that facilitates the ability to capture patterns and deduce qualitative information about multilayer data.

To give a concrete example, many researchers are interested in ranking the relative importance of nodes (and other network structures), which traditionally is accomplished using various ‘centrality’ measures. Centralities have been calculated for single-layer networks for several decades [1,37], and numerous notions of centrality are now also available for multilayer networks [41,44]. It is therefore necessary to develop visualization tools that make it possible to compare such a wealth of diagnostics to each other in a compact, meaningful way. For example, it is often worthwhile to focus attention on one descriptor and compare the values obtained in each layer separately to the values obtained from the multilayer network and its aggregations. This is easy to do using the *muxViz* software.

We will now illustrate our annular visualization (see Figs. 4, 6, 8 and 10) using the example of multilayer centrality measures. Suppose that we have different arrays of information, where one should think of each array as having resulted from the calculation of some centrality diagnostic on a multilayer network. We visualize each array using a ring. The angle indicates node identity (regardless of the layer or layers in which it occurs). We bin the centrality values—e.g. either linearly or logarithmically—and we assign a colour to each bin to encode its value. Both the type of binning and the colour scheme are customizable in *muxViz*. We place the rings concentrically, and one can determine both the ring order and ring thicknesses according to any desired criteria. For example, in the visualizations in the present paper, we determine the thickness of each ring according to its information content (which we

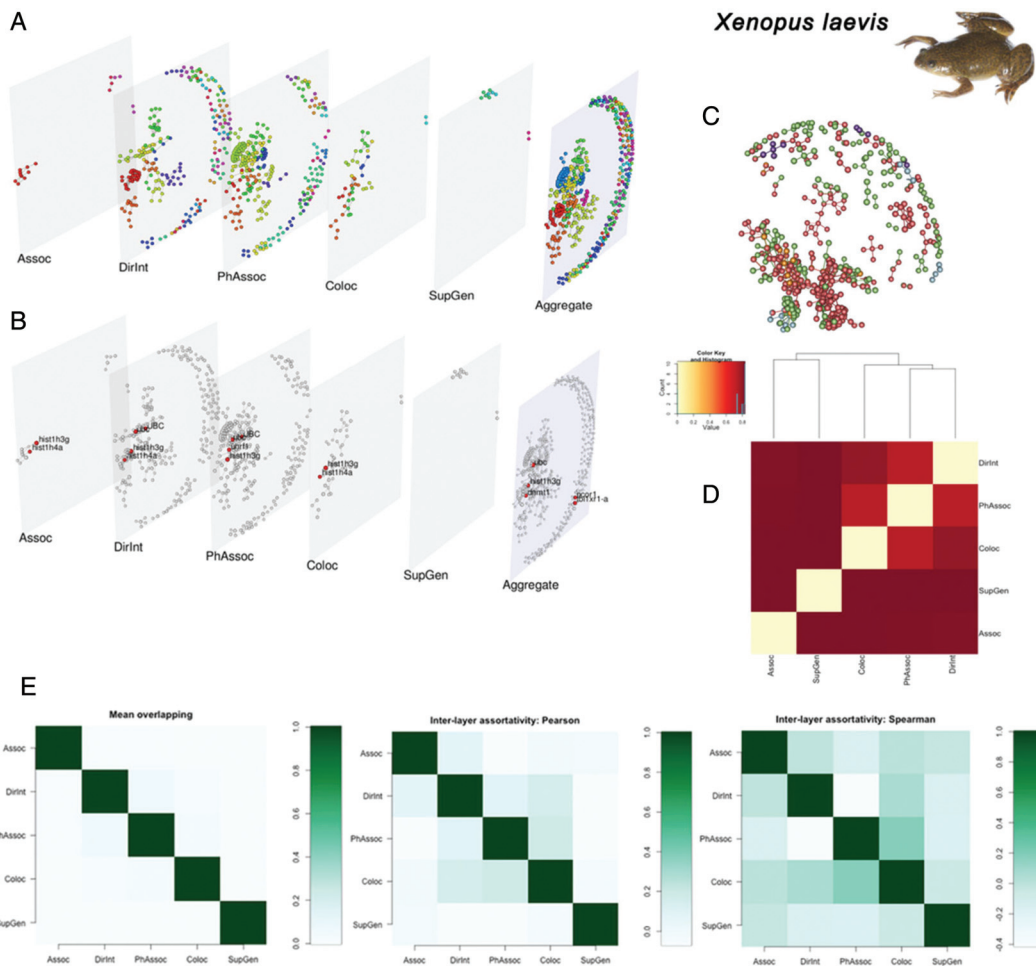


FIG. 3. Multilayer analysis of *X. laevis* genetic-interaction network. See Section 3.1 for details about each panel. [In this figure and all subsequent figures, we have purposely kept font sizes at muxViz's default level rather than increasing them.]

quantify using the Shannon information entropy of the distribution of the values): thinner rings have less information. Users can customize the order of the rings; in muxViz's default setting, it is determined automatically via hierarchically clustering. The muxViz software calculates a measure of correlation (e.g. Pearson, Spearman or JS divergence) between each pair of descriptors to obtain a set of pairwise distances, which we then hierarchically cluster to group the rings. This clustering procedure determines the order of the rings to try to maximize the readability of the annular plot.

One can also use the same principles when fixing some centrality descriptor and letting the rings correspond to the layers in a network, the multilayer network and an aggregated network (see Section 3). Such a plot might help to reveal, for instance, whether the large centrality of a node in a multilayer network is due primarily to its centrality value in a specific layer or if the aggregated network provides a reasonable proxy for such multilayer structure.

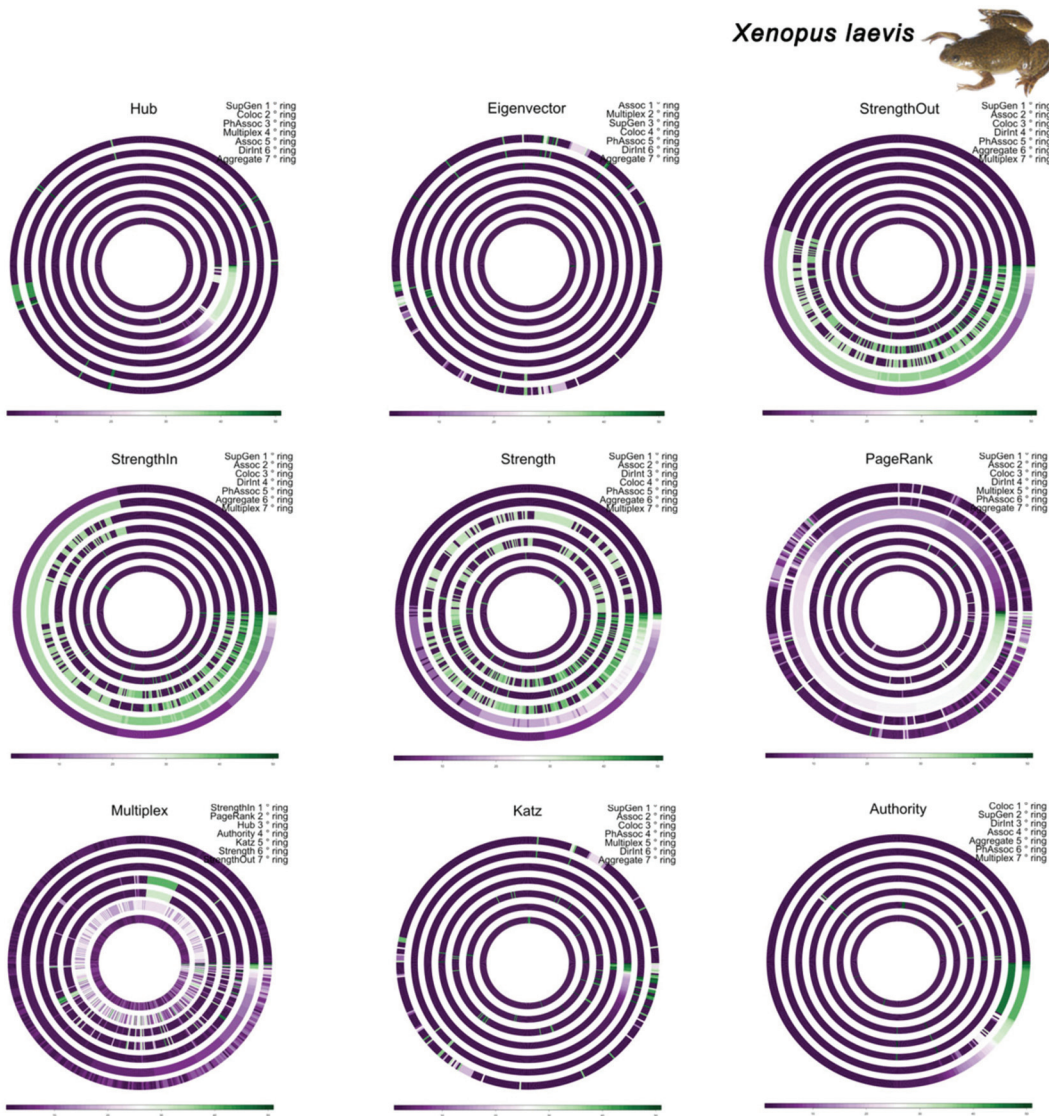


FIG. 4. Multilayer analysis (annular plots) of *X. laevis* genetic-interaction network. See Section 3.1 for details about each panel.

3. Analyses of empirical multilayer networks

To demonstrate the ability of muxViz to analyse and visualize multilayer networks, we consider different types of genetic interactions for organisms in the Biological General Repository for Interaction Datasets [69] ([BioGRID, thebiogrid.org](http://thebiogrid.org)), a public database that archives and disseminates genetic and protein interaction data from humans and model organisms. BioGRID currently includes more than 720,000 interactions that have been curated from both high-throughput data sets and individual focused studies using over 41,000 publications in the primary literature. We use BioGRID 3.2.108 (updated 1 January 2014). In this section, we focus on *Xenopus laevis* and show a network visualization in

Fig. 3(C). We give results of computations using *muxViz* in the other panels of Fig. 3. See Section 3.1 for other examples.

One can examine the global organization of nodes into modules (i.e. ‘communities’) through an algorithmic calculation of community structure [70,71]. For example, one can obtain dense communities in multilayer networks by optimizing a multilayer generalization of the modularity quality function [42]. To do this, one takes into account both intralayer and interlayer edges, and one seeks densely connected sets of nodes (i.e. communities) that are sparsely connected to each other when compared with some multilayer random-graph (null) model [41,42,60]. See Fig. 3(A) for a visualization of communities in *X. laevis* and Section 3.1 for other examples.

As we discussed previously, one can quantify the importance of a node by using various diagnostics to measure ‘centrality’. One calculates such a centrality (and a corresponding rank order) for each node by using multilayer generalizations of centrality measures [41,43,44]. The software *muxViz* has tools for calculating multilayer generalizations of several different types of centrality (e.g. degree, eigenvector [72], hub and authority [73], PageRank [74] and Katz [75]) either for an entire multilayer network or for each layer separately. As we illustrate in Fig. 3(B), centrality values (as well as other network measures) can be very different in multilayer networks than in their corresponding aggregations. Such results influence how one should interpret calculations of network measures for which genes or proteins are most important for activating or suppressing a given biological process, which people are most important in a social network, and so on. The data in question are multilayer, so the analysis of such data must take multilayer features into account [76].

Researchers are often also interested in considering a ‘compressed version’ of multilayer data sets that preserve as much information as possible without altering the primary descriptors. For such scenarios, it is possible to use the compression procedure discussed in Section 2.2 to identify the layers of a multilayer network that are providing redundant information [64] (see Fig. 3(D)).

In Fig. 3(E), we show three correlation measures for multilayer networks: (left) mean edge overlap, (centre) degree–degree Pearson correlation coefficient and (right) degree–degree Spearman correlation coefficient. In this example, the degree–degree Pearson and Spearman correlation coefficients between layers quantify the tendency of nodes to be hubs in different layers simultaneously. The *muxViz* software includes basic correlation measures; it is easy for users to add other diagnostics (such as the ones in [45]).

To summarize all of the information that one obtains from calculations like the ones above in a compact figure, we use an annular visualization (see Section 2.3) that facilitates the ability to capture patterns to deduce qualitative information about multilayer data. In Fig. 4 (see the panel labelled ‘Multiplex’), we show an example for centrality diagnostics, which measure the importance of nodes in various ways. Each ring indicates a centrality measure, and the angle determines the identity of a node in a network, regardless of the layer(s) in which it exists. One can use the same principles when fixing some centrality descriptor and letting the rings correspond to the layers in a network, the multilayer network and an aggregated network (see the other panels in Fig. 4). For the case of layers, one calculates a centrality measure for each layer separately without accounting for multilayer structure. For instance, it is evident that rings 3 (‘DirInt’ layer) and 5 (‘PhAssoc’ layer) are negatively correlated in the case of strength centrality because nodes tend to have opposite colours, whereas rings 6 (aggregated network) and 7 (multiplex network) are positively correlated, as expected for strength centrality. Our annular representation makes it easy to see similarity (or dissimilarity) in rank orderings according to different diagnostics. For example, their patterns reveal that physical association and direct interaction are dominant and determine the multilayer strength in the depicted example. In other cases (see Section 3.1), the ranking by some centrality measure in the multilayer network is poorly correlated to the ranking in either an

aggregated network or in individual layers separately. This underscores the value of using a multilayer framework for the calculation of the most central proteins (and, more generally, for determining which entities in complex systems are most important).

3.1 Analysis of other empirical multilayer networks

In this section, we present multilayer analyses of three additional biological systems to illustrate the power of muxViz. We examine the following examples:

- *C. elegans* connectome (see Figs. 5 and 6);
- *Herpes simplex* genetic-interaction network (see Figs. 7 and 8);
- *HIV-1* genetic-interaction network (see Figs. 9 and 10).

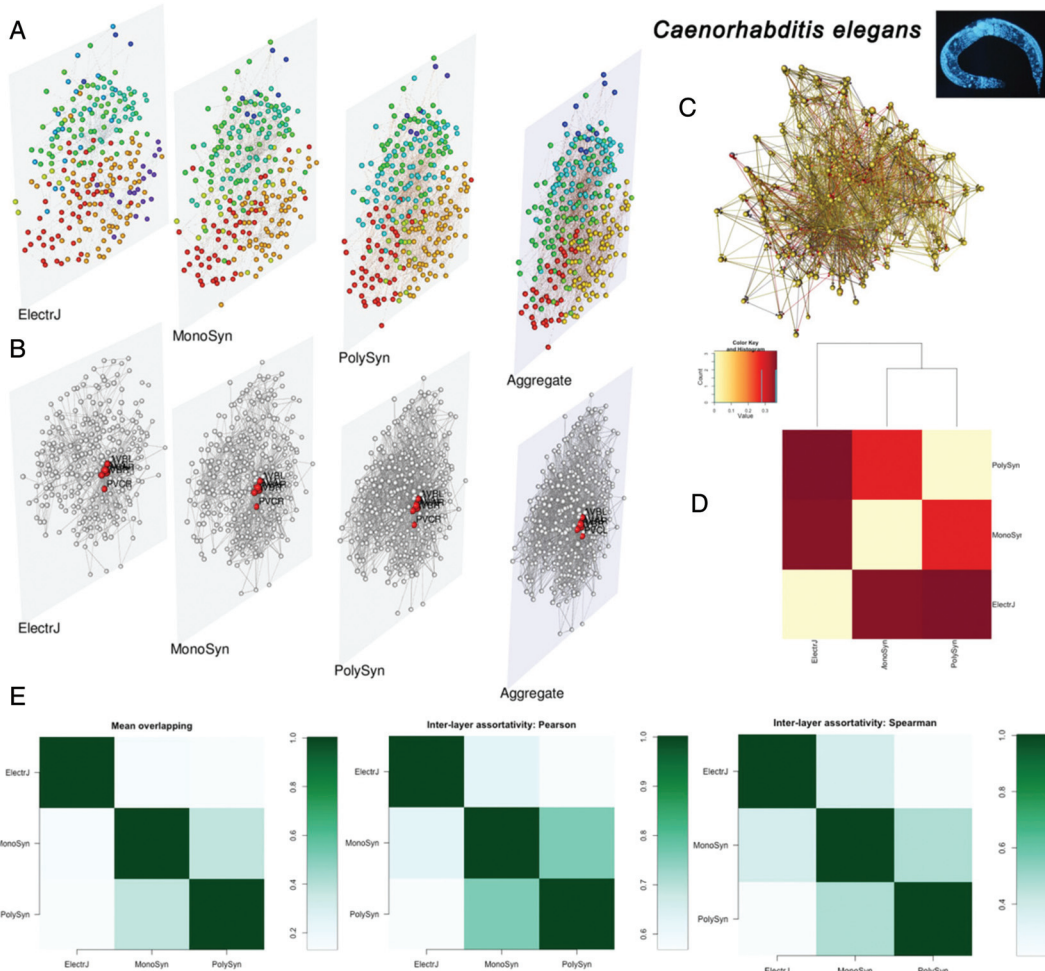


FIG. 5. Multilayer analysis of *C. elegans* connectome. See Section 3.1 for details about each panel.

As we did for the case of *X. laevis*, we include two figures for each example. In the first set of figures (see Figs. 5, 7 and 9), we show the following information:

- *Panel (A)*: Multilayer community structure from modularity maximization [42]. The colour of each node encodes its community assignment in a multilayer-network visualization. For comparison, we also show the results (and corresponding visualization) of community detection on an aggregated network, which we obtain by summing the corresponding intralayer edge weights of all layers. (In

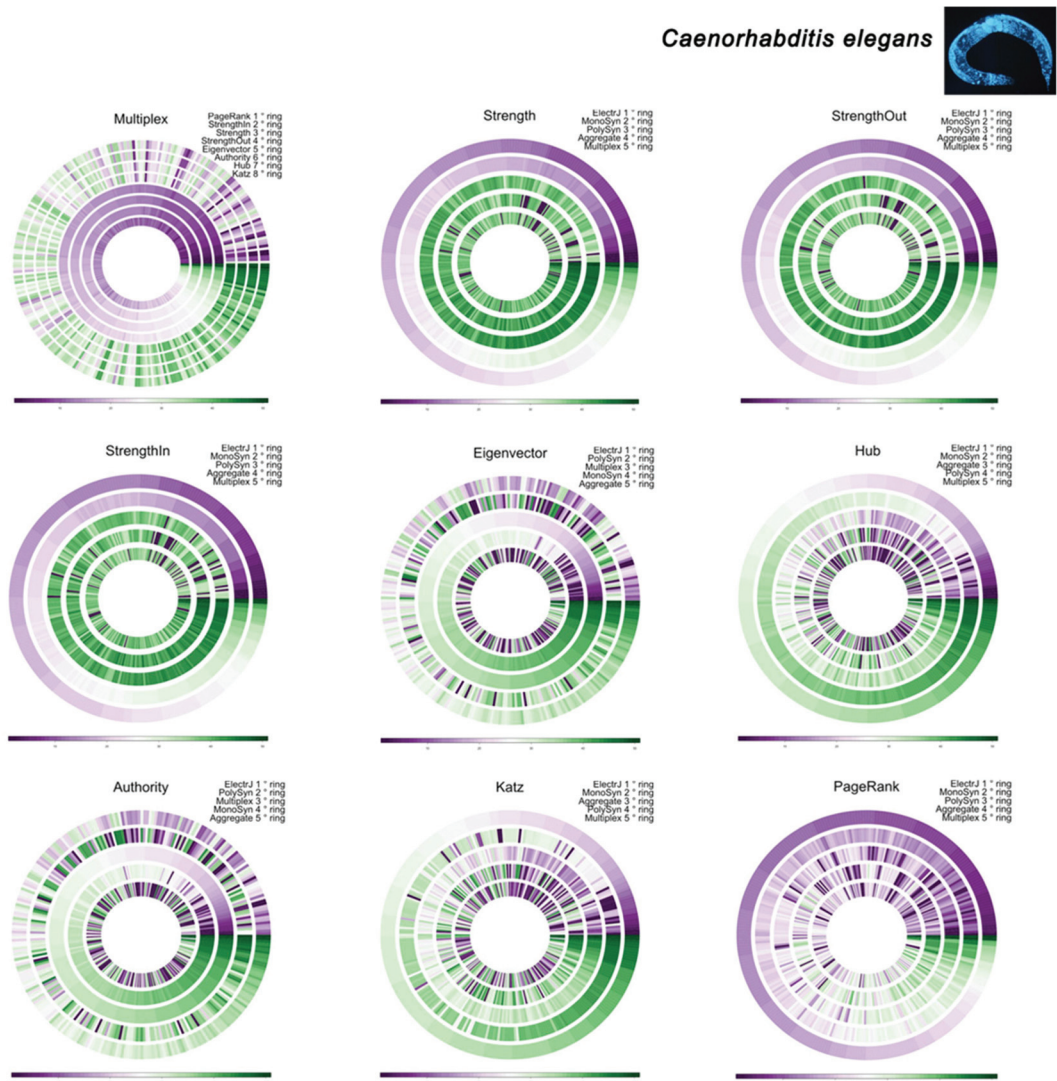


FIG. 6. Multilayer analysis (annular plots) of *C. elegans* connectome. See Section 3.1 for details about each panel.

other words, if A_{ij} gives the edge weight between nodes i and j on layer s , then we obtain an aggregated edge weight W_{ij} between nodes i and j by summing over s .)

- *Panel (B)*: Multilayer PageRank centrality [44]. We again use a multilayer-network visualization. We label the top five nodes from a ranking according to multilayer PageRank centrality. For comparison, we also show the results of PageRank centrality calculations on the aforementioned aggregated network.
- *Panel (C)*: Edge-coloured multigraph visualization of the network. We colour edges according to the layer to which they belong. We colour the nodes according to their layer (or layers); if a node exists on multiple layers, then we distribute its corresponding colours evenly.

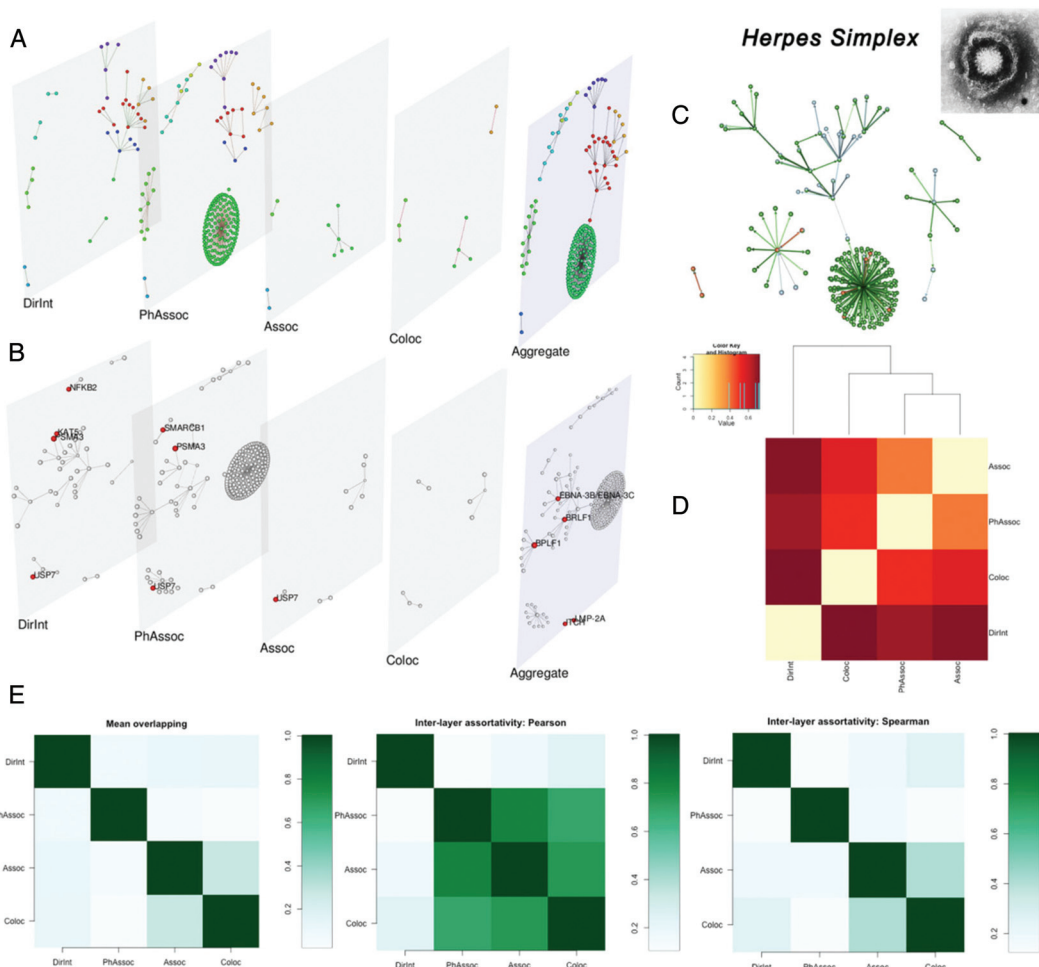


FIG. 7. Multilayer analysis of *H. simplex* genetic-interaction network. See Section 3.1 for details about each panel.

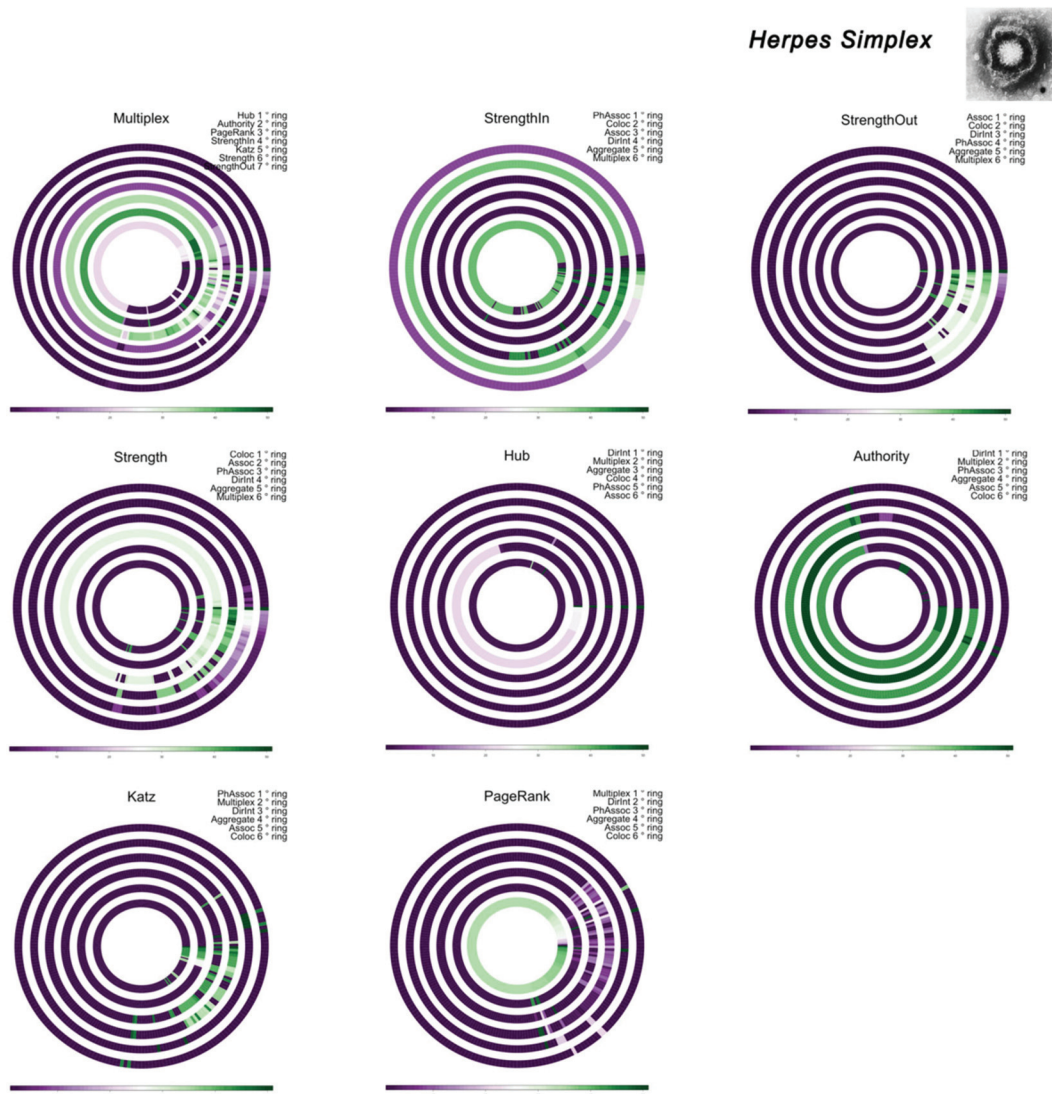


FIG. 8. Multilayer analysis (annular plots) of *H. simplex* genetic-interaction network. See Section 3.1 for details about each panel. Note that we do not show eigenvector centrality because one layer consists of a directed acyclic graph (for which eigenvector centrality is unilluminating [1]).

- *Panel (D)*: Compressibility, analysis and corresponding reducibility dendrogram [64]. We show the distance matrix and the corresponding dendrogram, which we obtain using Ward hierarchical clustering.
- *Panel (E)*: Measures of correlation between layers: (left) mean edge overlap, (centre) degree-degree Pearson correlation coefficient and (right) degree-degree Spearman correlation coefficient.

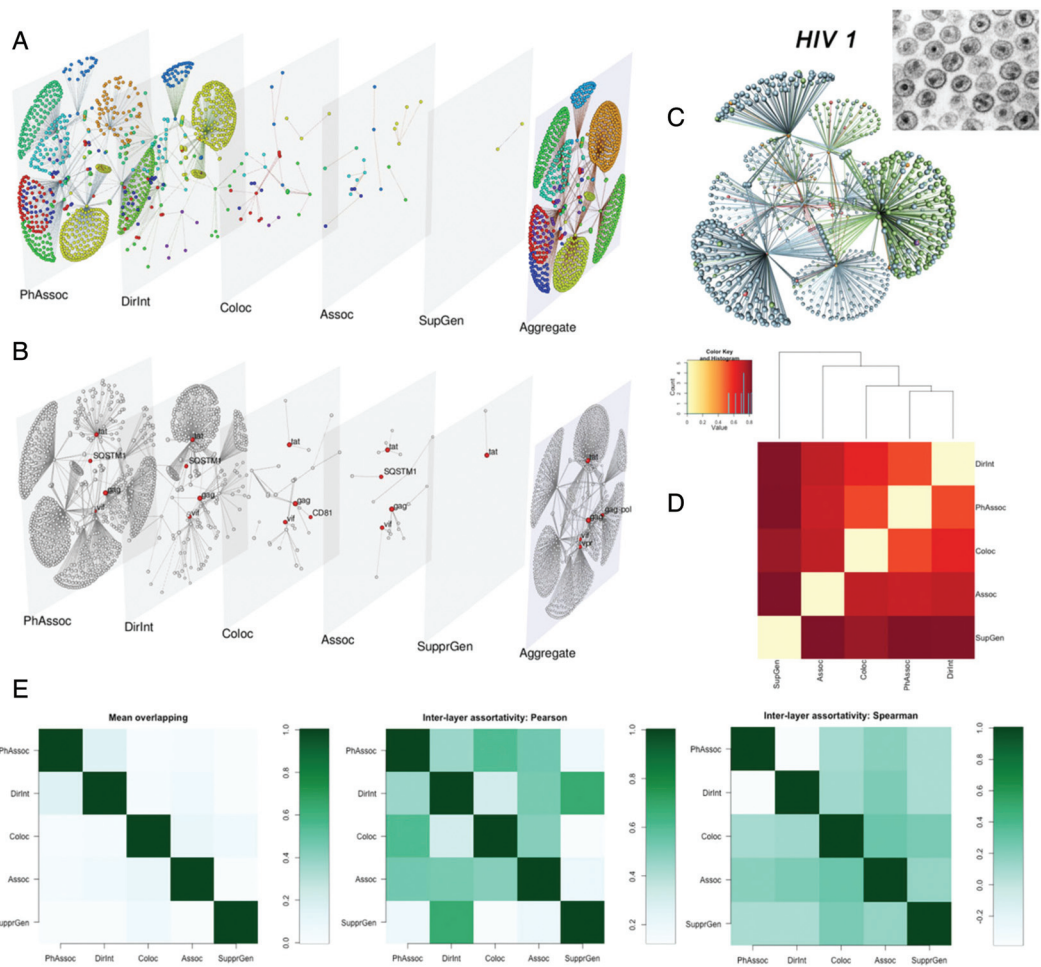


FIG. 9. Multilayer analysis of *HIV-1* genetic-interaction network. See Section 3.1 for details about each panel.

In the second set of figures (see Figs. 6, 8 and 10), we show our annular visualization for the centrality descriptors:

- In each panel titled ‘Multiplex’, we consider a multilayer network. Each ring corresponds to a different centrality descriptor.
- In the other panels, we consider a specific centrality descriptor (which we specify in the title of the panel). Each ring encodes the values of that descriptor, which we calculate in each layer separately. We also include rings for the calculation of the corresponding centrality diagnostic in the multilayer network and in its aggregation to a single-layer weighted network.

We specify the order of the rings in the list of labels on the right of each plot. In each case, the top label refers to the innermost ring and the bottom label refers to the outermost ring.

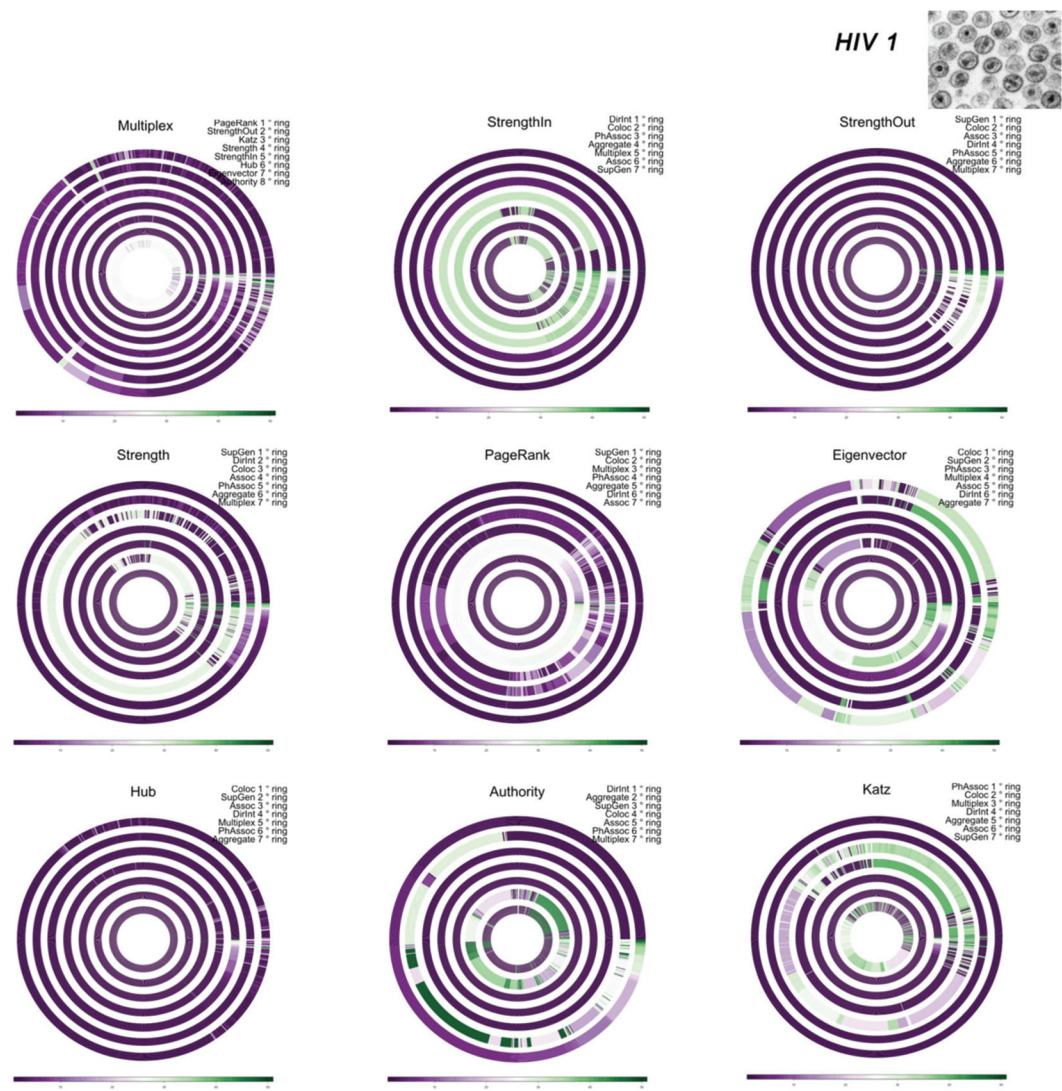


FIG. 10. Multilayer analysis (annular plots) of *HIV-1* genetic-interaction network. See Section 3.1 for details about each panel.

4. Conclusion

In the current era of ‘big data’, there is now an intense deluge of multilayer data. To avoid throwing away important information or obtaining misleading results, it is increasingly crucial to use methods that exploit multilayer structure. In this paper, we present new software and associated methodology that exploits the new paradigm of multilayer networks, and we illustrate how it can be used to analyse and visualize several examples. Our software, *muxViz*, provides an open-source framework for the

analysis of multilayer networks. Additionally, the modular structure of muxViz—along with its open-source license—makes it easy to add new methods. Moreover, although we have focused on examples of biological networks, muxViz is clearly also useful for multilayer networks from any other setting. As we illustrated in Fig. 2, it can even be overlaid over spatial information.

Acknowledgement

The authors thank Serafina Agnello for support with graphics.

Funding

All authors were supported by the European Commission FET-Proactive project PLEXMATH (Grant No. 317614; the project website is <http://www.plexmath.eu/>). A.A. also acknowledges the financial support from the Generalitat de Catalunya 2009-SGR-838, the ICREA Academia, and the James S. McDonnell Foundation. M.A.P. acknowledges a grant (EP/J001759/1) from the EPSRC.

REFERENCES

1. NEWMAN, M. E. J. (2010) *Networks: An Introduction*. Oxford: Oxford University Press.
2. KITANO, H. (2002) Computational systems biology. *Nature*, **420**, 206–210.
3. DE JONG, H. (2002) Modeling and simulation of genetic regulatory systems: a literature review. *J. Comput. Biol.*, **9**, 67–103.
4. BARABÁSI, A.-L. & OLTVAI, Z. N. (2004) Network biology: understanding the cell's functional organization. *Nat. Rev. Genet.*, **5**, 101–113.
5. SHARAN, R., ULITSKY, I. AND SHAMIR, R. (2007) Network-based prediction of protein function. *Mol. Syst. Biol.*, **3**, 88.
6. BEYER, A., BANDYOPADHYAY, S. & IDEKER, T. (2007) Integrating physical and genetic maps: from genomes to interaction networks. *Nat. Rev. Genet.*, **8**, 699–710.
7. SPORNS, O. (2014) Contributions and challenges for network models in cognitive neuroscience. *Nat. Neurosci.*, **17**, 652–660.
8. COLIZZA, V., BARRAT, A., BARTHÉLEMY, M. & VESPIGNANI, A. (2006) The role of the airline transportation network in the prediction and predictability of global epidemics. *Proc. Natl. Acad. Sci. USA*, **103**, 2015–2020.
9. GÓMEZ-GARDEÑES, J., CAMPILLO, M., FLORÍA, L. & MORENO, Y. (2007) Dynamical organization of cooperation in complex topologies. *Phys. Rev. Lett.*, **98**, 108103.
10. GÓMEZ-GARDEÑES, J., LATORA, V., MORENO, Y. & PROFUMO, E. (2008) Spreading of sexually transmitted diseases in heterosexual populations. *Proc. Natl. Acad. Sci. USA*, **105**, 1399–1404.
11. EAGLE, N., PENTLAND, A. S. & LAZER, D. (2009) Inferring friendship network structure by using mobile phone data. *Proc. Natl. Acad. Sci. USA*, **106**, 15274–15278.
12. LAZER, D., PENTLAND, A. S., ADAMIC, L., ARAL, S., BARABÁSI, A. L., BREWER, D., CHRISTAKIS, N., CONTRACTOR, N., FOWLER, J., GUTMANN, M., et al. (2009) Life in the network: the coming age of computational social science. *Science*, **323**, 721.
13. BALCAN, D., COLIZZA, V., GONÇALVES, B., HU, H., RAMASCO, J. J. & VESPIGNANI, A. (2009) Multi-scale mobility networks and the spatial spreading of infectious diseases. *Proc. Natl. Acad. Sci. USA*, **106**, 21484–21489.
14. KITSAK, M., GALLOS, L. K., HAVLIN, S., LILJEROS, F., MUCHNIK, L., STANLEY, H. E. & MAKSE, H. A. (2010) Identification of influential spreaders in complex networks. *Nat. Phys.*, **6**, 888–893.
15. ARAL, S. & WALKER, D. (2012) Identifying influential and susceptible members of social networks. *Science*, **337**, 337–341.

16. VESPIGNANI, A. (2012) Modelling dynamical processes in complex socio-technical systems. *Nat. Phys.*, **8**, 32–39.
17. JEONG, H., TOMBOR, B., ALBERT, R., OLTVAI, Z. N. & BARABÁSI, A.-L. (2000) The large-scale organization of metabolic networks. *Nature*, **407**, 651–654.
18. JEONG, H., MASON, S. P., BARABÁSI, A.-L. & OLTVAI, Z. N. (2001) Lethality and centrality in protein networks. *Nature*, **411**, 41–42.
19. SHEN-ORR, S. S., MILO, R., MANGAN, S. & ALON, U. (2002) Network motifs in the transcriptional regulation network of *Escherichia coli*. *Nat. Genet.*, **31**, 64–68.
20. MASLOV, S. & SNEPPEN, K. (2002) Specificity and stability in topology of protein networks. *Science*, **296**, 910–913.
21. TONG, A. H. Y., LESAGE, G., BADER, G. D., DING, H., XU, H., XIN, X., YOUNG, J., BERRIZ, G. F., BROST, R. L., CHANG, M., et al. (2004) Global mapping of the yeast genetic interaction network. *Science*, **303**, 808–813.
22. GUIMERÀ, R. & AMARAL, L. A. N. (2005) Functional cartography of complex metabolic networks. *Nature*, **433**, 895–900.
23. ROSENFIELD, N., YOUNG, J. W., ALON, U., SWAIN, P. S. & ELOWITZ, M. B. (2005) Gene regulation at the single-cell level. *Science*, **307**, 1962–1965.
24. CHEN, B. L., HALL, D. H. & CHKLOVSKII, D. B. (2006) Wiring optimization can relate neuronal structure and function. *Proc. Natl. Acad. Sci. USA*, **103**, 4723–4728.
25. GOH, K.-I., CUSICK, M. E., VALLE, D., CHILDS, B., VIDAL, M. & BARABÁSI, A.-L. (2007). The human disease network. *Proc. Natl. Acad. Sci. USA*, **104**, 8685–8690.
26. COSTANZO, M., BARYSHNIKOVA, A., BELLAY, J., KIM, Y., SPEAR, E. D., SEVIER, C. S., DING, H., KOH, J. L., TOUFIGHI, K., MOSTAFAVI, S., et al. (2010) The genetic landscape of a cell. *Science*, **327**, 425–431.
27. VAN VREESWIJK, C. & SOMPOLINSKY, H. (1996) Chaos in neuronal networks with balanced excitatory and inhibitory activity. *Science*, **274**, 1724–1726.
28. SPORNS, O. & KÖTTER, R. (2004) Motifs in brain networks. *PLoS Biol.*, **2**, e369.
29. BUZSÁKI, G. & DRAGUHN, A. (2004) Neuronal oscillations in cortical networks. *Science*, **304**, 1926–1929.
30. SPORNS, O., CHIALVO, D. R., KAISER, M. & HILGETAG, C. C. (2004) Organization, development and function of complex brain networks. *Trends Cognit. Sci.*, **8**, 418–425.
31. MANTINI, D., PERRUCCI, M. G., DEL GRATTA, C., ROMANI, G. L. & CORBETTA, M. (2007) Electrophysiological signatures of resting state networks in the human brain. *Proc. Natl. Acad. Sci. USA*, **104**, 13170–13175.
32. BULLMORE, E. & SPORNS, O. (2009) Complex brain networks: graph theoretical analysis of structural and functional systems. *Nat. Rev. Neurosci.*, **10**, 186–198.
33. SEELEY, W. W., CRAWFORD, R. K., ZHOU, J., MILLER, B. L. & GREICIUS, M. D. (2009) Neurodegenerative diseases target large-scale human brain networks. *Neuron*, **62**, 42–52.
34. BASSETT, D. S., WYMB, N. F., PORTER, M. A., MUCHA, P. J., CARLSON, J. M. & GRAFTON, S. T. (2011) Dynamic reconfiguration of human brain networks during learning. *Proc. Natl. Acad. Sci. USA*, **108**, 7641–7646.
35. NICOSIA, V., VALENCIA, M., CHAVEZ, M., DÍAZ-GUILERA, A. & LATORA, V. (2013) Remote synchronization reveals network symmetries and functional modules. *Phys. Rev. Lett.*, **110**, 174102.
36. NICOSIA, V., VÉRTES, P. E., SCHAFER, W. R., LATORA, V. & BULLMORE, E. T. (2013) Phase transition in the economically modeled growth of a cellular nervous system. *Proc. Natl. Acad. Sci. USA*, **110**, 7880–7885.
37. WASSERMAN, S. & FAUST, K. (1994) *Social Network Analysis: Methods and Applications*. Cambridge: Cambridge University Press.
38. BOCCALETTI, S., LATORA, V., MORENO, Y., CHAVEZ, M. & HWANG, D.-U. (2006) Complex networks: structure and dynamics. *Phys. Rep.*, **424**, 175–308.
39. BARTHÉLEMY, M. (2011) Spatial networks. *Phys. Rep.*, **499**, 1–101.
40. HOLME, P. & SARAMÄKI, J. (2012) Temporal networks. *Phys. Rep.*, **519**, 97–125.
41. KIVELÄ, M., ARENAS, A., BARTHELEMY, M., GLEESON, J. P., MORENO, Y., & PORTER, M. A. (2014) Multilayer networks. *J. Complex Netw.*, **2**, 203–271.

42. MUCHA, P. J., RICHARDSON, T., MACON, K., PORTER, M. A. & ONNELA, J.-P. (2010) Community structure in time-dependent, multiscale, and multiplex networks. *Science*, **328**, 876–878.
43. DE DOMENICO, M., SOLÉ-RIBALTA, A., COZZO, E., KIVELÄ, M., MORENO, Y., PORTER, M. A., GÓMEZ, S. & ARENAS, A. (2013) Mathematical formulation of multilayer networks. *Phys. Rev. X*, **3**, 041022.
44. DE DOMENICO, M., SOLÉ-RIBALTA, A., OMODEI, E., GÓMEZ, S. & ARENAS, A. (2013) Centrality in interconnected multilayer networks. Pre-print, arXiv:1311.2906.
45. NICOSIA, V. & LATORA, V. (2014) Measuring and modelling correlations in multiplex networks. Pre-print, arXiv:1403.1546.
46. BATTISTON, F., NICOSIA, V. & LATORA, V. (2014) Structural measures for multiplex networks. *Phys. Rev. E*, **89**, 032804.
47. BULDYREV, S. V., PARSHANI, R., PAUL, G., STANLEY, H. E. & HAVLIN, S. (2010) Catastrophic cascade of failures in interdependent networks. *Nature*, **464**, 1025–1028.
48. BRUMMITT, C. D., D'SOUZA, R. M. & LEICHT, E. (2012) Suppressing cascades of load in interdependent networks. *Proc. Natl. Acad. Sci. USA*, **109**, E680–E689.
49. LEE, K.-M., KIM, J. Y., CHO, W.-K., GOH, K. & KIM, I. (2012) Correlated multiplexity and connectivity of multiplex random networks. *New J. Phys.*, **14**, 033027.
50. RADICCHI, F. & ARENAS, A. (2013) Abrupt transition in the structural formation of interconnected networks. *Nat. Phys.*, **9**, 717–720.
51. CARDILLO, A., GÓMEZ-GARDEÑES, J., ZANIN, M., ROMANCE, M., PAPO, D., DEL POZO, F. & BOCCALETI, S. (2013) Emergence of network features from multiplexity. *Sci. Rep.*, **3**, 1344.
52. COZZO, E., KIVELÄ, M., DE DOMENICO, M., SOLÉ-RIBALTA, A., ARENAS, A., GÓMEZ, S., PORTER, M. A. & MORENO, Y. (2013) Clustering coefficients in multiplex networks. Pre-print, arXiv:1307.6780.
53. CELLAI, D., LÓPEZ, E., ZHOU, J., GLEESON, J. P. & BIANCONI, G. (2013) Percolation in multiplex networks with overlap. *Phys. Rev. E*, **88**, 052811.
54. YAĞAN, O. & GLIGOR, V. (2012) Analysis of complex contagions in random multiplex networks. *Phys. Rev. E*, **86**, 036103.
55. GÓMEZ-GARDEÑES, J., REINARES, I., ARENAS, A. & FLORÍA, L. M. (2012) Evolution of cooperation in multiplex networks. *Sci. Rep.*, **2**, 620.
56. COZZO, E., ARENAS, A. & MORENO, Y. (2012) Stability of Boolean multilevel networks. *Phys. Rev. E*, **86**, 036115.
57. COZZO, E., BAÑOS, R. A., MELONI, S. & MORENO, Y. (2013) Contact-based social contagion in multiplex networks. *Phys. Rev. E*, **88**, 050801.
58. DE DOMENICO, M., SOLÉ-RIBALTA, A., GÓMEZ, S. & ARENAS, A. (2014) Navigability of interconnected networks under random failures. *Proc. Natl. Acad. Sci. USA*, **111**, 8351–8356.
59. DELELLIS, P., DI BERNARDO, M., GOROCHEWSKI, T. E. & RUSSO, G. (2010) Synchronization and control of complex networks via contraction, adaptation and evolution. *IEEE Circuits Syst. Mag.*, **10**, 64–82, Third quarter.
60. BASSETT, D. S., PORTER, M. A., WYMBS, N. F., GRAFTON, S. T., CARLSON, J. M. & MUCHA, P. J. (2013) Robust detection of dynamic community structure in networks. *Chaos*, **23**, 013142.
61. FRUCHTERMAN, T. M. & REINGOLD, E. M. (1991) Graph drawing by force-directed placement. *Softw. Practice Exper.*, **21**, 1129–1164.
62. KAMADA, T. & KAWAI, S. (1989) An algorithm for drawing general undirected graphs. *Inf. Process. Lett.*, **31**, 7–15.
63. LIMA, A., DE DOMENICO, M., PEJOVIC, V. & MUOLESI, M. (2013) Exploiting cellular data for disease containment and information campaigns strategies in country-wide epidemics. Pre-print, arXiv:1306.4534.
64. DE DOMENICO, M., NICOSIA, V., ARENAS, A. & LATORA, V. (2014) Layer aggregation and reducibility of multilayer interconnected networks. Pre-print, arXiv:1405.0425.
65. MAJTEY, A., LAMBERTI, P. & PRATO, D. (2005) Jensen–Shannon divergence as a measure of distinguishability between mixed quantum states. *Phys. Rev. A*, **72**, 052310.

66. BRAUNSTEIN, S. L., GHOSH, S. & SEVERINI, S. (2006) The Laplacian of a graph as a density matrix: a basic combinatorial approach to separability of mixed states. *Ann. Comb.*, **10**, 291–317.
67. BRIËT, J. & HARREMOËS, P. (2009) Properties of classical and quantum Jensen–Shannon divergence. *Phys. Rev. A*, **79**, 052311.
68. GAN, G., MA, C. & WU, J. (2007) *Data Clustering: Theory, Algorithms, and Applications*. Philadelphia: SIAM.
69. STARK, C., BREITKREUTZ, B.-J. REGULY, T., BOUCHER, L., BREITKREUTZ, A. & TYERS, M. (2006) Biogrid: a general repository for interaction datasets. *Nucleic Acids Res.*, **34**(Suppl. 1), D535–D539.
70. PORTER, M. A., ONNELA, J.-P. & MUCHA, P. J. (2009) Communities in networks. *Not. Am. Math. Soc.*, **56**, 1082–1097, 1164–1166.
71. FORTUNATO, S. (2010) Community detection in graphs. *Phys. Rep.*, **486**, 75–174.
72. BONACICH, P. (1972) Factoring and weighting approaches to status scores and clique identification. *J. Math. Sociol.*, **2**, 113–120.
73. KLEINBERG, J. M. (1999) Authoritative sources in a hyperlinked environment. *J. ACM*, **46**, 604–632.
74. BRIN, S. & PAGE, L. (1998) The anatomy of a large-scale hypertextual web search engine. *Comput. Netw. ISDN Sys.*, **30**, 107–117.
75. KATZ, L. (1953) A new status index derived from sociometric analysis. *Psychometrika*, **18**, 39–43.
76. BOCCALETI, S., BIANCONI, G., CRIADO, R., DEL GENIO, C. I., GÓMEZ-GARDEÑES, J., ROMANCE, M., SENDÍÑA-NADAL, I., WANG, Z., & ZANIN, M. (2014) The structure and dynamics of multi-layer networks. Available at <http://www.sciencedirect.com/science/article/pii/S0370157314002105> (see also <http://arxiv.org/abs/1407.0742>).

Appendix: Technical details about muxViz

We developed muxViz using R (<http://www.r-project.org/>), a free and widely-adopted framework for statistical computing, and GNU Octave (<https://www.gnu.org/software/octave/>), an open-source high-level interpreted language that is intended primarily for numerical computations. The Octave language is very similar to the proprietary environment MATLAB (<http://www.mathworks.es/products/matlab/>), and one can import the code to MATLAB in a straightforward manner. The muxViz software requires R 3.0.2 (or above) and Octave 3.4.0 (or above). The official webpage for muxViz is <http://muxviz.net>, where additional material (such as tutorials for its installation and usage) is available.

The muxViz framework is a free and open-source package for the analysis and the visualization of multilayer networks. It is released under GNU General Public License version 3 (<https://www.gnu.org/copyleft/gpl.html>) and exploits R to provide an easy and accessible user interface for the visualization of networks, the calculation of network diagnostics, and the visual representation of the results of calculations. Specifically, R allows the construction of a graphical user interface (GUI), which can be used either locally (client-side software) or via the internet (remote Web server), and an Octave library that we developed performs calculations of matrices and tensors.

Using muxViz is simple and does not require any programming skill; one can do all computations and visualization via the user interface. Additionally, because of muxViz's modular structure, users can also create their own modules for calculating new diagnostics and for customizing visual representations.

The muxViz framework allows both two-dimensional and three-dimensional visualizations of networks. The latter exploits OpenGL technology, so users can interactively change the perspective and navigate a network. We show representative static snapshots of such interactive visualizations in Fig. 1(B and D) and in panel (C) of Figs. 3, 5, 7 and 9.